

# Prediction of Ductile Fracture in Metal Blanking

A. M. Goijaerts

e-mail: ad@wfw.wtb.tue.nl

L. E. Govaert

F. P. T. Baaijens

Materials Technology,  
Eindhoven University of Technology,  
P.O. Box 513,  
5600 MB Eindhoven, The Netherlands

*This study is focused on the description of ductile fracture initiation, which is needed to predict product shapes in the blanking process. Two approaches are elaborated using a local ductile fracture model. According to literature, characterization of such a model should take place under loading conditions, comparable to the application. Therefore, the first approach incorporates the characterization of a ductile fracture model in a blanking experiment. The second approach is more favorable for industry. In this approach a tensile test is used to characterize the fracture model, instead of a complex and elaborate blanking experiment. Finite element simulations and blanking experiments are performed for five different clearances to validate both approaches. In conclusion it can be stated that for the investigated material, the first approach gives very good results within the experimental error. The second approach, the more favorable one for industry, yields results within 6 percent of the experiments over a wide, industrial range of clearances, when a newly proposed criterion is used. [S1087-1357(00)02202-4]*

## 1 Introduction

Blanking is a common technique in high volume production. Since the beginning of this century, researchers have been analyzing the blanking process. Blanking experiments on either planar [1,2] or axisymmetric [3–5] configurations have led to empirical guidelines for process variables such as punch and die radius, speed and clearance. Nevertheless, the blanking process is not yet fully understood.

Nowadays, it can be observed that product specifications are getting more severe, since high-tech products are becoming smaller and smaller. This can lead to lengthy trial and error procedures in developing industrial blanking applications and a proper model of the blanking process is desired. Because of the constantly changing loading situations in the material, the process is too complex for an analytical approach [6–8]. Instead, the finite element method has been used to simulate the blanking process, with varying success [9–11]. One major difficulty in the numerical analysis is the description of ductile fracture. This is important because ductile fracture initiation determines the fracture zone and shear zone and thus the product shape (Fig. 1).

The physical background for ductile fracture in metals is known to be the initiation, growth and coalescence of voids [12–14]. Voids can initiate at inclusions, secondary phase particles or at dislocation pile-ups. Growth and coalescence of voids are driven by plastic deformation. Therefore, it seems evident to incorporate the deformation history in a ductile fracture model. Because the numerical implementation of a fracture growth model, using a local ductile fracture model, is present in our research group [11], this category of criteria will be utilized for this purpose.

The class of local ductile fracture criteria that incorporate the stress and strain history (a short overview is given by Clift et al., [15]) can be written as an integral over plastic strain ( $\epsilon_p$ ) up to fracture of a certain function of the actual stress state (reflected by the Cauchy stress tensor  $\sigma$ ) reaching a threshold value  $C$ :

$$\int_{\epsilon_p} f(\sigma) d\epsilon_p = C \quad (1)$$

If the integral on the left-hand side reaches the critical value  $C$  during the process, ductile fracture is supposed to initiate. In the formulations for the different criteria, some parameters that influence ductile fracture are expected to appear: plastic strain and

triaxiality (triaxiality is defined as hydrostatic stress over equivalent Von Mises stress:  $\sigma_h/\bar{\sigma}$ ). A larger hydrostatic pressure postpones the initiation of voids and slows down the growth of voids. Therefore, triaxiality is often represented in  $f(\sigma)$ . Large plastic strains permit voids to grow and coalesce. This justifies the integration over plastic strain.

In the formulation of Eq. (1),  $C$  is stated to be a material constant and has to be determined experimentally. However, in literature no example is found, where  $C$  is determined in an experiment which is in a very different loading condition from the verification configuration. These kinds of criteria are only found successful when applied in similar loading conditions, which suggests that some information of the loading path is represented in the parameter  $C$ . Therefore, the approach where  $C$  is determined in the blanking process is expected to be the most successful. However, for industrial applications this is a rather complicated and difficult

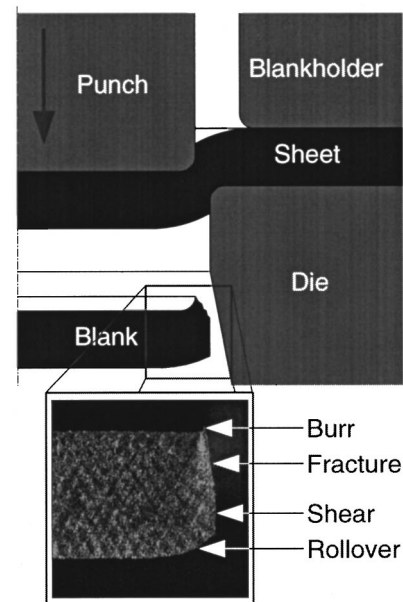


Fig. 1 The blanking process with an indication of the different zones determining the product shape

Contributed by the Manufacturing Engineering Division for publication in the JOURNAL OF MANUFACTURING SCIENCE AND ENGINEERING. Manuscript received April 1999; revised Oct 1999. Associate Technical Editor: K. Stelson

**Table 1 Material properties of X30Cr13**

Young's Modulus	$1.87 \cdot 10^5$ MPa
Poisson's Ratio	0.28
Yield Strength	420 MPa

approach. An industrially favorable approach would be to determine the  $C$  in an easier test, e.g., a tensile test. Both approaches will be elaborated in this paper.

In section 2 we discuss the experimental methods and the numerical model. In section 3 we determine the parameter  $C$  in a blanking experiment. In section 4 we try the other approach, where we attempt to predict ductile fracture initiation in the blanking process by determining the parameter  $C$  in a tensile test. Finally, we discuss the results and conclude in section 5.

## 2 Methods

**2.1 Experimental.** In order to obtain a satisfying material description, also for large plastic strains, we used a material characterization technique, that had already been presented [16,17] and is briefly explained in subsection 2.1.1.

To characterize and verify ductile fracture initiation criteria of the form of Eq. (1), experiments are needed. For the first approach we need an axisymmetric blanking setup with different geometries (subsection 2.1.2). We chose to vary the clearance, because the effect on the product shape of a change in clearance is known to be large [3–5].

For the second approach a universal tensile testing machine is required to characterize ductile fracture criteria in tensile tests. To verify the validity of fracture models in tensile tests for different levels of triaxiality, an additional setup is needed to perform tensile tests under hydrostatic pressure (subsection 2.1.3).

**2.1.1 Material Characterization.** We used a 13 percent Cr. ferritic stainless steel (X30Cr13, DIN 17006), that was assumed to plastically deform according the Von Mises yield condition with isotropic hardening [18]. (Some material properties are given in Table 1.) In formulating this plastic deformation, the yield stress increases with increasing equivalent plastic strain. The relationship between the yield stress and the equivalent plastic strain is difficult to obtain experimentally for large strains, using conventional test such as tensile or shear experiments. This was achieved by performing 20 tensile tests with each tensile specimen being subjected to a different amount of rolling to obtain different initial plastic deformations. The assumption of isotropic hardening allows addition of the rolling and tensile equivalent plastic strains. We determined the relationship between the yield stress and the

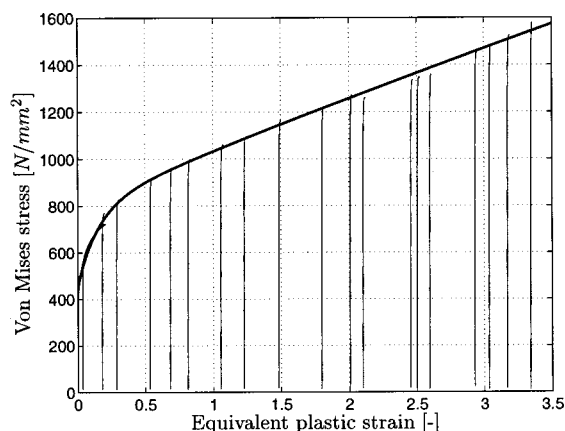


**Fig. 2 Strain hardening behavior**

equivalent plastic strain, by fitting a master-curve through the maxima of the stress-strain curves of these tensile tests (Fig. 2). This fitting procedure yields the following master-curve:

$$\sigma_y = 420 + 133 \cdot (1 - e^{-\epsilon_p^{0.0567}}) + 406 \cdot (\epsilon_p)^{0.5} + 70.7 \cdot \epsilon_p \quad (2)$$

where  $\sigma_y$  is the Von Mises yield stress and  $\epsilon_p = (2/3 \cdot (\epsilon_1^2 + \epsilon_2^2 + \epsilon_3^2))^{0.5}$  is the equivalent logarithmic plastic strain, with  $\epsilon_1, \epsilon_2, \epsilon_3$  the principal strains.

**2.1.2 Blanking Experiments.** An axisymmetric blanking setup with a die-hole diameter of 10.00 mm, including a blankholder with constant pressure, was built with five different punches (diameters: 9.98, 9.94, 9.88, 9.80 and 9.70 mm) resulting in five different clearances, covering the industrially used range of clearances (1, 3, 6, 10 and 15 percent of the sheet thickness of 1 mm). To avoid exorbitant simulation times, the punch and die radii are enlarged to approximately 0.1 mm. The punch radii are somewhat smaller and the die radius is a bit larger, to make sure fracture will initiate at the punch and grow to the die radius. We want to determine the punch displacements at fracture initiation ( $a+b+c$ , Fig. 3) experimentally, to have reference points in the numerical simulations for the initiation of ductile fracture. In our blanking setup, six experiments were performed for every clearance. The shear zone or burnish ( $b$ ) and the burr ( $c$ ) are measured afterwards at eight positions over the circumference of the blanked products, and averaged to justify for the misalignment of the punch. Then, the values are averaged over the six experiments and the standard-deviation is calculated (Fig. 3).

It was shown by Stegeman et al. [18] that the roll-over or draw-in ( $a$ ) could be accurately predicted for this material, with the mentioned, validated model. Because it is difficult to account for the spring-back of the specimen, the roll-over is taken from the numerical simulations and not from an experimental measurement. Such determination of the roll-over applies for other materials as well, if the numerical finite element model describes the roll-over accurately. The element size near the transition of roll-over and shear zone is taken as the standard-deviation. The results are in agreement with the trend found in literature [1] and depicted in Fig. 3.

The roll-over height is very low for small clearances and becomes larger for wider clearances because the broader deformation zone allows more bending. The shear zone is getting smaller for larger clearances and this is caused by the hydrostatic stress state; for small clearances the hydrostatic pressure is larger and this postpones ductile fracture initiation, despite of the fact that the deformation is more localized and that the strains are larger.

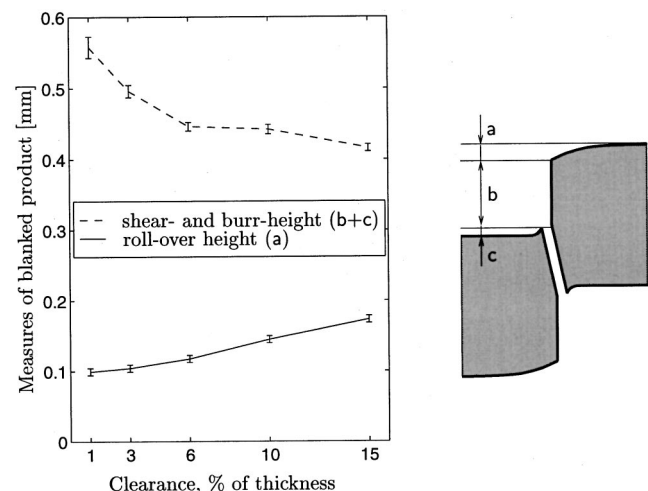


**Fig. 3 Experimental results for ductile fracture initiation for varying clearance**

The burr height is very small (in the order of  $5 \mu\text{m}$ ) and is largely determined by the punch radius. The average punch displacements at fracture ( $a+b+c$ ) is firstly plotted in Fig. 6 (later), along with twice the standard deviations (95 percent interval). The combination of the trend for roll-over height and shear height (plus burr) explains the minimum in the curve. There is a small experimental deviation for the clearance of 10 percent. This is a result of the larger punch radius for the specific 10 percent clearance punch. A larger punch radius postpones ductile fracture initiation because the deformation becomes less localized.

**2.1.3 Tensile Tests Under Different Pressures.** An experimental setup is used, with which it is possible to perform a tensile test under a superposed hydrostatic stress. The tensile test is performed in an oil chamber and the oil pressure is maintained during the entire tensile test. Measurements are performed at three different levels of superposed hydrostatic pressure: 0, 250 and 500 MPa. Clamp force and displacement are measured. The dimensions of the tensile specimens are chosen according to the requirements of the pressurized tensile apparatus and shown in Fig. 4.

The measured force displacement curves were identical within the experimental error for all different hydrostatic pressures. This means that the hydrostatic pressure has no influence on the plastic yielding and hardening behavior. This is an experimental approval for the use of a yield condition without pressure dependence. However, a closer investigation of the broken tensile specimens showed a significant difference; the thickness of the material at the neck after fracture was smaller for larger hydrostatic pressures. This means that the process of necking was interrupted by ductile fracture in an earlier stage under a smaller hydrostatic pressure. Results are shown in Fig. 5 along with twice the standard-deviations (95 percent interval) for three measurements at every hydrostatic pressure. This can be explained by considering the influence of the triaxiality ( $\sigma_h/\bar{\sigma}$ ) on the physical mechanism of ductile fracture initiation, being the initiation, growth and coalescence of voids. The triaxiality is greatly influenced by the hydrostatic pressures because they are in the same order of mag-

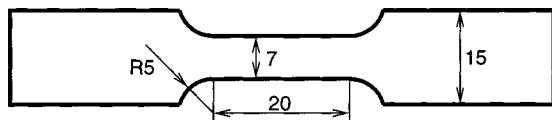


Fig. 4 Dimensions of the tensile specimens in mm, thickness is 1 mm

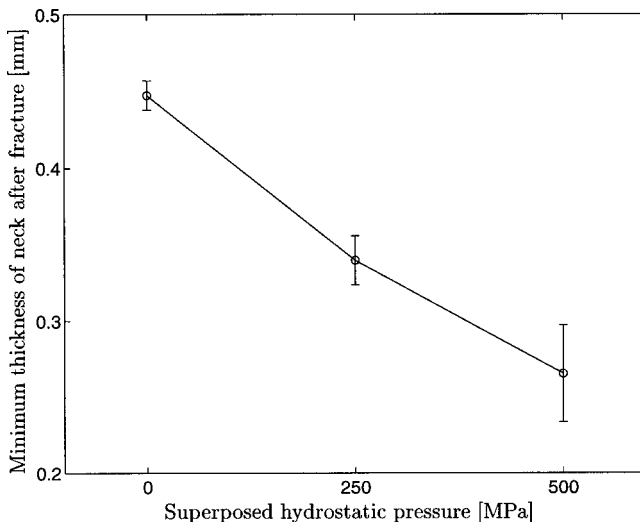


Fig. 5 Minimum thickness of neck after fracture as a function of hydrostatic pressure

nitude as the equivalent Von Mises stresses. A larger hydrostatic pressure, or a more negative hydrostatic stress, makes the triaxiality more negative and postpones ductile fracture initiation. One can imagine that voids inside the material will not initiate or grow that fast if there is a large hydrostatic pressure. Thus, there will be more plastic deformation in the neck, and thus larger local strains, for lower triaxialities (higher hydrostatic pressures).

**2.2 Numerical.** We simulated the blanking process using a two-dimensional, axisymmetric finite element model, described by Brokken et al. [17] and Stegeman et al. [18]. Quasi-static analyses are performed on the model geometries that match the experimental setup for the five different clearances. We modelled the specimen with an isotropic elasto-plastic material, using the material properties as specified in subsection 2.1.1. The plastic material behavior is described by the Von Mises yield condition, by isotropic hardening and by the Prandtl-Reuss representation of the flow rule [19]. The mesh, used for the 15 percent clearance, is shown in Fig. 8. The left boundary at the top (specimen center) is the axis of symmetry. The other boundaries are either free surfaces or in interaction with a contacting body (punch, die or blankholder).

Linear quadrilateral elements are used, which become smaller as they approach either the die radius or the punch radius. Near those radii, which are between 0.05 and 0.15 mm, the element proportions need to be in the range of  $5 \mu\text{m}$ , resulting in up to 3000 elements in the entire mesh. This element size is not necessary to predict the process force correctly, but it will be vital to accurately describe the field variables, needed to predict ductile fracture initiation. The punch moves down and penetrates the specimen, resulting in constantly changing boundary conditions. To deal with these difficult boundary conditions and the localized large deformations, the finite element application that we used, combines three numerical procedures: the commercial implicit finite element package MARC [19] (using an updated Lagrange formulation), an arbitrary Lagrange-Euler approach [20,21] and an automatic remeshing algorithm [17], to overcome severe mesh distortion problems. This model was experimentally validated *up to fracture* on both deformation fields—using Digital Image Correlation—and process forces, using a planar blanking setup [18,22]. Therefore, the deformation history in the blanking process can be calculated adequately, which is a prerequisite for the *local* modelling of ductile fracture.

### 3 Characterization of a Ductile Fracture Model in Blanking

In subsection 3.1 the strategy to characterize a ductile fracture model in the blanking process and subsequently predict ductile fracture initiation over a wide range of clearances is explained. Next, some ductile fracture criteria, found in literature, are evaluated and some adaptations are made to make two models valid for the blanking process.

**3.1 Strategy.** We consider ductile fracture initiation criteria of the form of Eq. (1). The right-hand side of this formulation is meant to be a material constant. With the *Characterization of a ductile fracture model* we mean: the determination of the material parameter  $C$ . This is done by experimentally determining the punch displacement for one clearance at fracture initiation and simulating this blanking process up to that point of fracture initiation. During this simulation not only the usual state variables are stored, but also the left-hand side of Eq. (1) is stored as a field variable. When the experimental punch displacement at fracture is reached in the simulation,  $C$  is determined to be the maximum value of  $\int f(\sigma)d\epsilon_p$  over the entire FEM mesh, and at this point we declare the criterion to be *characterized*. The parameter  $C$  should then be valid for any clearance.

If a ductile fracture initiation model is characterized, we can evaluate the validity of it for the blanking process over the entire range of clearances. This evaluation is performed using FEM

simulations of the blanking process for the other clearances. During the simulations  $\int f(\sigma)d\epsilon_p$  is stored as a field variable and as soon as this field variable reaches the critical  $C$ , the punch displacement at fracture is predicted. If the predicted punch displacements for all clearances are within the experimental error, a proper ductile fracture initiation model for the blanking process is found (for this material).

**3.2 Application of Ductile Fracture Models.** A large number of ductile fracture initiation criteria, taken from literature, are evaluated according to the explained strategy. A selection of some good and some special ones are discussed here and mentioned in Table 2. The plastic work criterion is based on the assumption that the material can only absorb a certain amount of energy. This energy criterion was proposed in this form by Freudenthal [23]. The Cockcroft & Latham [24] criterion considers the effect of the maximum principal stress ( $\sigma_1$ ) over the plastic strain path. Maximum principal stresses are often used in linear elastic fracture mechanics to describe brittle fracture. This criterion has already been used for the blanking process by several authors [25–27]. The [...] notation of Eq. (3) is used here to make sure that the fracture integral cannot decrease for a growing equivalent plastic strain.

$$[x] = \begin{cases} x, & x > 0 \\ 0, & x \leq 0 \end{cases} \quad (3)$$

This assumption is similar to the thermodynamically based theory in damage mechanics that damage cannot decrease. The Rice & Tracey criterion is based on a theoretical study of the growth of a void in an infinite rigid, perfect plastic matrix. The Oyane criterion is derived from a plasticity theory for porous materials, assuming that the volumetric strain has a critical level. In this criterion a second parameter  $A_O$  was inserted, which gives more freedom to find a valid ductile fracture model. (This parameter is proposed as a material constant by Oyane et al., [28]).

For the evaluation of these criteria, the 15 percent clearance experiment was taken as the reference experiment in which the  $C$  is determined. For the other clearances the displacement at fracture initiation is predicted and results are shown for the criteria with only one parameter in Fig. 6. The plastic work or energy criterion predicts fracture initiation completely wrong. For the smallest clearance a punch displacement of only 0.39 mm is predicted. The Cockcroft & Latham criterion, that was already used for the blanking process, does not predict the trend correctly; the punch displacement at fracture for a small clearance should be larger than for a wide clearance. The Rice & Tracey [29] criterion gives comparable results.

To achieve better results the influence of triaxiality on ductile fracture initiation should be changed for the blanking process. For the Rice & Tracey criterion this is easily realized by varying the constant  $A_{RT} = 3/2$ . If this constant becomes a parameter, the criterion starts to resemble the Oyane criterion. The adapted Rice & Tracey criterion ( $A_{RT} = 3/2$  is changed into  $A_{RT} = 2.9$ ) and the Oyane criterion ( $A_O = 3.9$ ) yield good results that are presented in Fig. 7. In Fig. 8 the value of the Oyane integral is drawn as a field variable in the 15 percent-experiment at the punch displacement, where experimentally fracture initiation was detected. The maximum value is located just next to the punch radius and this is in good agreement with the position that was experimentally found.

**Table 2 Four ductile fracture initiation criteria, selected from literature**

Plastic Work [23]	$\int_{\epsilon_p} \bar{\sigma} d\epsilon_p = C$
Cockcroft and Latham [24]	$\int_{\epsilon_p} [\sigma_1] d\epsilon_p = C$
Rice and Tracey [29], $A_{RT} = 3/2$	$\int_{\epsilon_p} \exp(A_{RT} \cdot \sigma_h / \bar{\sigma}) d\epsilon_p = C$
Oyane et al. [28]	$\int_{\epsilon_p} [1 + A_O \cdot \sigma_h / \bar{\sigma}] d\epsilon_p = C$

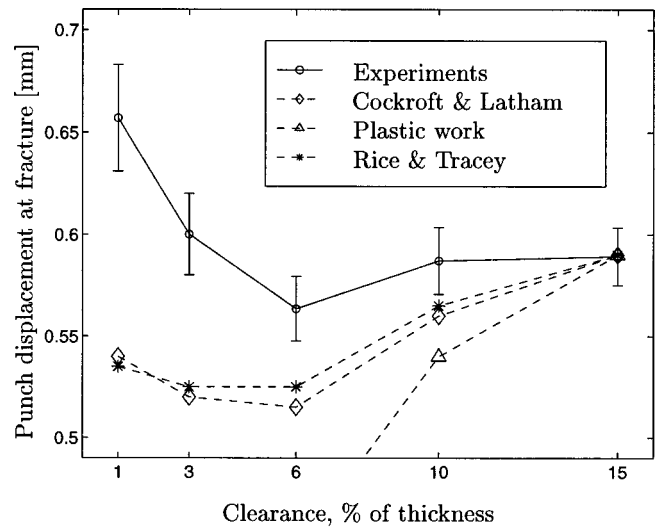


**Fig. 6 The evaluation of three criteria from literature with one parameter. The critical values  $C$  are determined in the 15 percent-experiment; Cockcroft & Latham:  $C = 1.40 \cdot 10^3$  [MPa]; Plastic work:  $C = 3.49 \cdot 10^3$  [MPa]; Rice & Tracey,  $C = 2.32$  [–].**

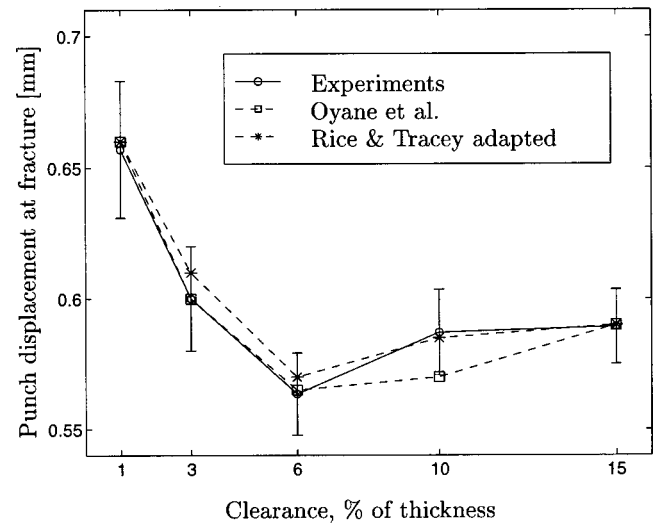


**Fig. 7 Results for the adapted Rice & Tracey and Oyane criterion**

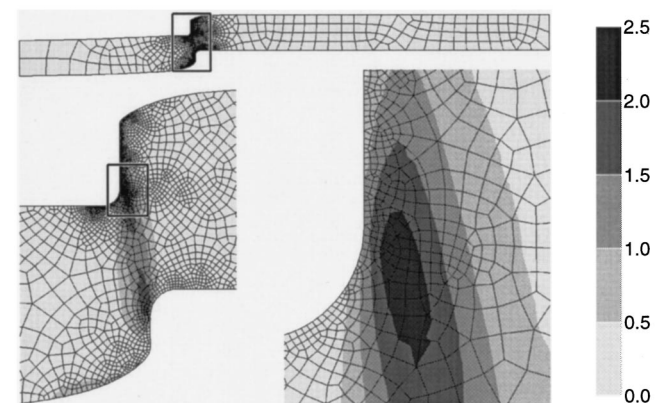


**Fig. 8 Field variable plot of the Oyane integral for an axisymmetric blanking model, at the punch displacement where fracture initiated (15 percent clearance), with two zoomed plots. Maximum value is 2.38. The location of the maximum is in agreement with experimental results.**

**Table 3 Two ductile fracture initiation criteria, valid for the blanking process**

Rice & Tracey, adapted: $A_{RT}=2.9$	$\int_{\epsilon_p} \exp(A_{RT} \cdot \sigma_h / \bar{\sigma}) d\epsilon_p = C$
Oyane et al. [28], $A_O=3.9$	$\int_{\epsilon_p} [1 + A_O \cdot \sigma_h / \bar{\sigma}] d\epsilon_p = C$

If the  $C$  is determined in another blanking experiment (with another clearance) its value will appear to be approximately the same. The two criteria that can predict ductile fracture initiation in the blanking process over a wide range of clearances by performing only one blanking experiment are summarized in Table 3. The constants  $C$  are determined to be 2.76 and 2.38 in the 15 percent experiment, for the Rice & Tracey and the Oyane criterion, respectively.

#### 4 Characterization of a Ductile Fracture Model in the Tensile Test

For industrial applications it would be a great advantage if a fracture criterion could be characterized by performing an easy test, instead of a complicated and difficult, well-conditioned, blanking experiment. In this section the application of the tensile test to characterize a ductile fracture criterion is elucidated.

Firstly, the strategy to predict ductile fracture in blanking, using a tensile test, is explained. Then, the simulation of tensile tests under different hydrostatic pressures along with the results are described. Finally, some criteria are evaluated and a new criterion is proposed because the existing criteria are not valid for both blanking and tensile tests under different hydrostatic pressures.

**4.1 Strategy.** The strategy to predict ductile fracture in blanking will be the following: firstly, a tensile test is performed, at room pressure, and the thickness of the neck after fracture is measured. Then, the tensile test has to be simulated up to the point where this thickness of the neck is reached. (This is the point of fracture initiation.) This simulation provides the deformation history of the tensile test, with which the  $C$  of a ductile fracture criterion can be determined. Finally, the characterized ductile fracture criterion can be applied to the blanking process for a specific geometry; during the simulation of this blanking process  $\int f(\sigma) d\epsilon_p$  is stored as a field variable and as soon as this field variable reaches the critical  $C$ , the punch displacement at fracture is predicted. In this paper this approach will be verified over the entire range of clearances.

During the search for a valid ductile fracture initiation criterion, an extra intermediate verification is performed; the critical parameter  $C$  should also be valid for tensile tests at different hydrostatic pressures. If a criterion does not fulfill this requirement it is rejected, because the influence of hydrostatic pressure on ductile fracture should be accounted for correctly.

**4.2 Simulation of Tensile Tests Under Different Hydrostatic Pressures.** A tensile test is simulated with an FEM computation, using the material data presented in subsection 2.1.1. The Von Mises yield condition is used, in which the hydrostatic stress component has no influence on the yielding behavior. Thus, the calculated force displacement curve for the tensile test is independent of the hydrostatic pressures. This was already experimentally observed in subsection 2.1.3. Therefore, only one FEM-simulation is required to obtain the stress and strain history for

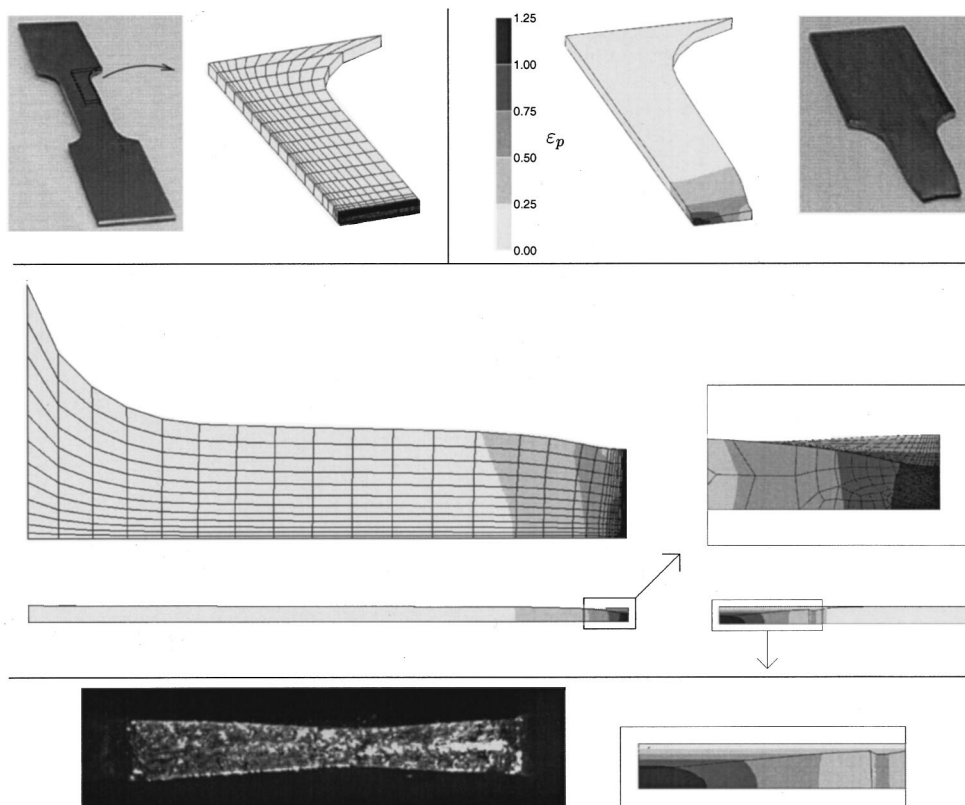


**Fig. 9 Simulation of a tensile test and experimental verification on deformations. In the upper left corner the undeformed tensile specimen is shown with the modelled part(1/8). Upper right, the calculated deformations at fracture initiation are shown with five levels of the equivalent plastic strain. In the center, the three orthogonal views of the deformed specimen are shown with a zoomed plot of the refined mesh in the neck. At the bottom, the experimental fracture surface is compared with the calculated cross-sectional area in the neck at fracture initiation. (Mind the wedge-like shape.)**

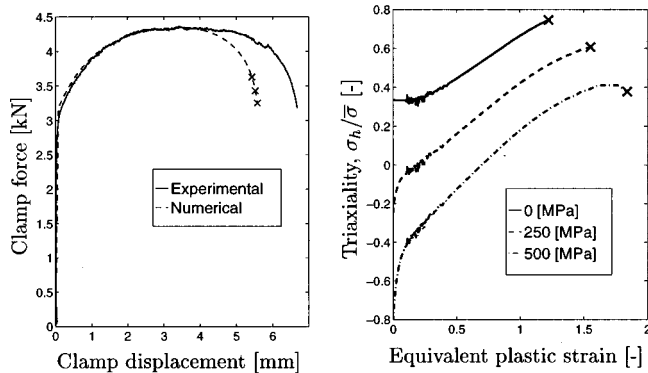


**Fig. 10 The numerical and experimental force displacement curves (left plot). The crosses are the points where the experimental thickness of the neck after fracture is numerically reached for the three different hydrostatic pressures. In the right plot the deformation history of the overall center of the specimen up to the point of fracture initiation (crosses) is presented for the tensile tests under different hydrostatic pressures.**

tensile tests under different hydrostatic pressures. This is because the stress state can be compensated afterwards for the hydrostatic pressure. A three-dimensional calculation is needed to simulate the necking process correctly. No imperfection needs to be modelled to initiate the neck due to the chosen boundary conditions.

The modelled tensile specimen, the initial mesh, the deformed mesh and the fractured specimen are all shown in Fig. 9. It can be seen that the FEM-model predicts the deformation of the tensile specimen well. Also the wedge-like shape of the specimen at fracture is predicted correctly. The photograph of the fractured surface and the FEM-simulation show that the highest plastic deformation is located at the overall center of the specimen. That this center point is also the point of fracture initiation can be shown by putting the two fractured halves of the tensile specimen back together. They do not fit perfectly because a gap exists in the middle; after fracture initiation in the center, there was still some plastic deformation at the edges.

Besides this verification on deformation behavior, the FEM-simulation is also checked on the force displacement curve. The experimental and numerical force displacement curves are depicted in the left-hand side of Fig. 10. The only difference between experiment and FEM-simulation is the point of necking. This point is completely determined by the shape of the master-curve for the hardening behavior of Eq. (2). FEM-calculations demonstrated that if the master-curve was slightly changed, the numerical point of necking could vary substantially so that the numerical clamp displacement became even larger as in the experiment. We chose to stick with the master-curve, determined in subsection 2.1.1. The error made in the description of the deformation history, due to this choice, is very small. This can be demonstrated at the hand of Fig. 10. In the plot of the triaxiality versus equivalent plastic strain for the three different hydrostatic pressures (plotted in the right-hand side of Fig. 10), the homogeneous deformation should have lasted a bit longer; the straight part for the 0 MPa curve at a triaxiality of 1/3, is experimentally a negligibly tiny part larger. The triaxiality plots for the hydrostatic pressures of 250 and 500 MPa are deduced from the calculated one for 0 MPa. (The wrinkles on the plots are caused by numerical difficulties to initiate the neck, because no imperfection was used to activate the necking process.)

Now the needed information, to characterize ductile fracture criteria in a tensile test and apply them on the blanking process, is present. Also, the validity of criteria for tensile tests over a range of superimposed hydrostatic pressures can be checked.

### 4.3 Application of Ductile Fracture Models, Using a Tensile Test.

The idea is to characterize a ductile fracture initiation model in a tensile test and use this characterized model to predict punch displacement at fracture initiation in the blanking process. Of all examined criteria, two were found to be valid for the blanking process in section 3. These criteria of Table 3 are now tested with this procedure. The first step is to determine the  $C$  in the tensile test with room pressure (0 MPa). Where the  $C$ 's were determined to be 2.76 and 2.38 respectively for the adapted Rice & Tracey and Oyane and Oyane criterion in the blanking process, now, in the tensile tests, the  $C$ 's are determined to be 5.76 and 3.64. This resulted for the adapted Rice & Tracey criterion in an over-prediction of the punch displacement at fracture of more than 30 percent, and for the Oyane criterion the deviations were within 25 percent. Moreover, both criteria were not able to predict ductile fracture initiation for the tensile tests under hydrostatic pressure within satisfying margins as is shown in Fig. 11. From these results it can be concluded that the criteria of Table 3 cannot describe ductile fracture initiation for both tensile tests under different hydrostatic pressures *and* blanking, for this specific material. Therefore, they are rejected.

Because no criterion has been found that satisfies this procedure, we propose a new one:

$$\int_{\varepsilon_p} [1 + A_G \cdot \sigma_h / \bar{\sigma}] \varepsilon_p^{B_G} d\varepsilon_p = C \quad (4)$$

This criterion incorporates the triaxiality influence of the Oyane criterion (Table 3) but also the equivalent plastic strain is inserted in the integral. Therefore, the formulation  $f(\sigma)$  of Eq. (1) is now changed to  $f(\sigma, \varepsilon^p)$ , with  $\varepsilon^p$  the logarithmic plastic strain tensor. Mathematically, this means that the integral will grow faster for larger strains. Physically, this seems reasonable because at larger strains the dislocation density will be larger. Therefore, the void initiation is expected to be larger for larger plastic strains.  $A_G$  is equal to  $A_O (= 3.9)$  and  $B_G$  is found to be 0.63 to yield a valid criterion that describes ductile fracture initiation for both blanking and tensile tests under different hydrostatic pressures. The  $C$  is determined to be 3.53 in the tensile test at room pressure. The results for the other tensile tests are plotted in Fig. 12. For the 250 MPa experiment the deviation is below 10 percent and the prediction falls within the experimental error for the 500 MPa experi-

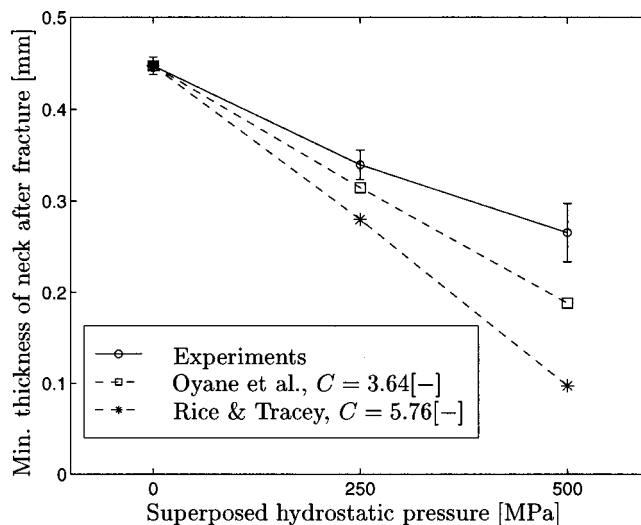


**Fig. 11 Validity check in the pressurized tensile tests for the criteria that performed well with a characterization in the blanking process (Table 3). Rice & Tracey and Oyane et al. deviate respectively 60 percent and 30 percent from the 500 MPa experiment, when the  $C$  is determined in the experiment at room pressure.**

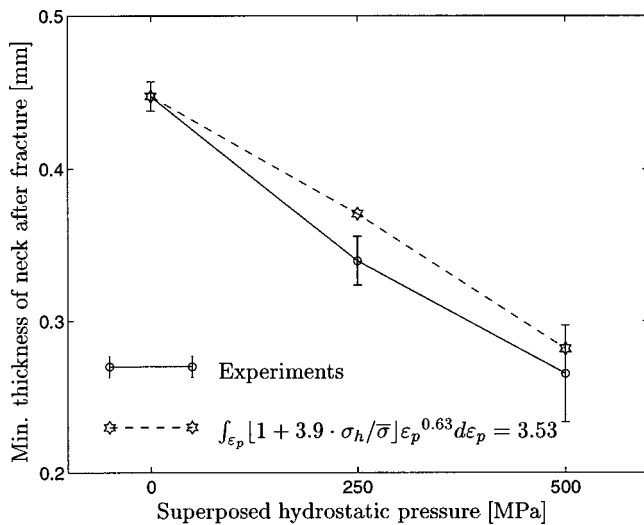


Fig. 12 Validity check of the proposed criterion for the tensile tests

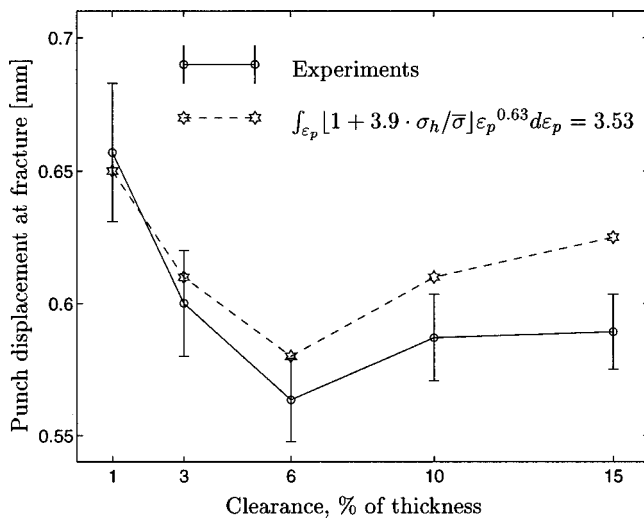


Fig. 13 Validity check of the proposed criterion for the blanking process

ment. The  $C$ , determined in the 0 MPa tensile test, is used to predict fracture initiation in blanking and results are depicted in Fig. 13. Not all results fall in the experimental range of twice the standard deviation, but the largest deviation of the predicted punch displacement at fracture is 6 percent.

It can be concluded that this criterion produces satisfying results in this procedure for this material. Therefore, it is possible to predict the punch displacement at fracture initiation over a wide range of clearances, by performing one tensile test.

## 5 Discussion and Conclusion

The goal of this research was to predict the product shape of a blanked product. An FEM-model, validated on the deformations in the blanking process, existed but the problem of ductile fracture initiation had not been solved yet. The category of *local* ductile fracture criteria was chosen for this application. For the characterization of such a model two approaches are discussed in this paper. To verify these approaches an experimental setup was built and results are presented for the punch displacement at ductile fracture initiation for five different clearances in the blanking process.

The approach that is expected to give the best results, considering literature, is the characterization of a fracture model *in the blanking process*. The two criteria of Table 3 produce good results if the influence of triaxiality on ductile fracture initiation has been determined. This means that in an industrial environment the product shape can be predicted for this material over a large range of clearances by performing only one blanking experiment, in which the critical  $C$  is determined.

The second approach is the characterization of the fracture model in an easier tensile test. Because existing criteria do not provide satisfying results, we have proposed a new criterion in Eq. (4). This criterion is not derived from a physical background but it incorporates parameters that are known to be important for ductile fracture initiation. In Fig. 13, it is shown that this criterion can predict ductile fracture initiation over a wide range of clearances if the critical  $C$  is determined in a tensile test. Furthermore, this criterion can predict ductile fracture initiation in tensile tests for different hydrostatic pressures. This is important because it shows that the criterion can predict fracture for a greatly varying triaxiality, which is known to be an important parameter for ductile fracture initiation. This approach yields satisfying results and is of course the more favorable for industry.

The question remains, whether these approaches will also be valid for other materials. If the formulation of the integral does not depend on the material (If  $A_{RT}$  and  $A_O$  in Table 3 and  $A_G$  and  $B_G$  in Eq. (4) are no material parameters), both approaches will be valid for other materials as well. The only material parameter will then be the critical  $C$ . However, this will have to be checked in future research, where these approaches will be tested for different materials [30]. If, for example, the multiplier in front of the triaxiality in the Oyane criterion,  $A_O$ , will appear to be a material parameter an extra blanking experiment will be needed in the first approach to determine this parameter and characterize the ductile fracture initiation model completely.

The influence of speed on the blanking process is not investigated in the present paper. For this reason, blanking and tensile speeds are chosen such that similar strain rates are obtained in all experiments. Preliminary results show a significant but small influence of blanking speed on the process force, and no effect of the speed was observed on the product shape of the blanked edge. A more profound investigation of the effect of punch speed on the blanking process will be presented in a future publication [31].

## Acknowledgments

This research was funded by the Dutch innovative research projects (IOP-C.94.702.TU.WB). Jan Post of Philips DAP/LTM kindly supplied the material and some data for the material model. Alan Duckett of the IRC in Polymer Science and Technology at the Leeds University is gratefully acknowledged for his help with the pressurized tensile experiments.

## Nomenclature

- $\sigma$  = Cauchy stress tensor, MPa
- $\sigma_h$  = hydrostatic stress,  $\sigma_h = 1/3 \cdot (\sigma_1 + \sigma_2 + \sigma_3)$  with  $\sigma_1, \sigma_2, \sigma_3$  the principal stresses, MPa
- $\sigma_y$  = momentary Von Mises yield stress (history parameter dependent on  $\epsilon_p$ ), MPa
- $\bar{\sigma}$  = equivalent Von Mises stress  $\bar{\sigma} = (1/2 \cdot [(\sigma_1 - \sigma_2)^2 + (\sigma_2 - \sigma_3)^2 + (\sigma_3 - \sigma_1)^2])^{0.5}$ , MPa
- $\sigma_1$  = maximum principal stress, MPa
- $\sigma_h / \bar{\sigma}$  = triaxiality
- $\epsilon_p$  = equivalent logarithmic plastic strain  $\epsilon_p = (2/3 \cdot (\epsilon_1^2 + \epsilon_2^2 + \epsilon_3^2))^{0.5}$  with  $\epsilon_1, \epsilon_2, \epsilon_3$  the principal strains
- $C$  = critical value of fracture model
- $A_O$  = parameter in Oyane model
- $A_{RT}$  = parameter in Rice & Tracey model
- $A_G$  = parameter in newly proposed model
- $B_G$  = parameter in newly proposed model

## References

- [1] Chang, T., and Swift, H., 1950, "Shearing of Metal Bars," *J. Inst. Met.*, **78**, pp. 119–146.
- [2] Atkins, A., 1981, "Surfaces Produced by Guillotining," *Philos. Mag.*, **43**, pp. 627–641.
- [3] Chang, T., 1951, "Shearing of Metal Blanks," *J. Inst. Met.*, **78**, pp. 393–414.
- [4] Johnson, W., and Slater, R., 1967, "A Survey of the Slow and Fast Blanking of Metals at Ambient and High Temperatures," *Proceedings of the International Conference of Manufacturing Technology*, Michigan, pp. 773–851.
- [5] Choy, C., and Balendra, R., 1996, "Experimental Analysis of Parameters Influencing Sheared-Edge Profiles," *Proceedings of the 4th International Conference on Sheet Metal*, Twente, pp. 101–110.
- [6] Noble, C., and Oxley, P., 1963, "Crack Formation in Blanking and Piercing," *Int. J. Prod. Res.*, **2**, pp. 265–274.
- [7] Fukui, S., Konda, K., and Maeda, K., 1971, "Smooth Shearing by Stepped Profile Tool," *Ann. CIRP*, **20**, pp. 57–58.
- [8] Zhou, Q., and Wierzbicki, T., 1996, "A Tension Zone Model of Blanking and Tearing of Ductile Metal Plates," *Int. J. Mech. Sci.*, **38**, pp. 303–324.
- [9] Post, J., and Voncken, R., 1996, FEM analysis of the punching process, *Proceedings of the 4th International Conference on Sheet Metal*, Twente, pp. 159–169.
- [10] Taupin, E., Breitting, J., Wu, W.-T., and Altan, T., 1996, "Materials Fracture and Burr Formation in Blanking; Results of FEM Simulations and Comparison with Experiments," *J. Mater. Process. Technol.*, **59**, pp. 68–78.
- [11] Brokken, D., Brekelmans, W., and Baaijens, F., 1998, "Numerical Modelling of the Metal Blanking Process," *J. Mater. Process. Technol.*, **83**, pp. 192–199.
- [12] Broek, D., 1971, A study on ductile failure, Ph.D. thesis, Delft University of Technology, The Netherlands.
- [13] Dodd, B., and Bai, Y., 1987, *Ductile Fracture and Ductility—With Applications to Metalworking*, Academic Press, London.
- [14] Bolt, P. J., 1989, Prediction of ductile failure, Ph.D. thesis, Eindhoven University of Technology, The Netherlands.
- [15] Clift, S., Hartley, P., Sturgess, C., and Rowe, G., 1990, "Fracture Prediction in Plastic Deformation Processes," *Int. J. Mech. Sci.*, **32**, pp. 1–17.
- [16] Swinden, T., and Bolsover, G., 1927, "Some Notes on Cold-Rolled Strip Steel," *J. Iron Steel Inst.*, London, **115**, pp. 569–602.
- [17] Brokken, D., Goijaerts, A., Brekelmans, W., Oomens, C., and Baaijens, F., 1997, "Modeling of the Blanking Process," *Computational Plasticity, Fundamentals and Applications*, Vol. 2, Barcelona, pp. 1417–1424.
- [18] Stegeman, Y., Goijaerts, A., Brokken, D., Brekelmans, W., Govaert, L., and Baaijens, F., 1999, "An Experimental and Numerical Study of a Planar Blanking Process," *J. Mater. Process. Technol.*, **87**, pp. 266–276.
- [19] MARC, 1998, MARC Manual: Volume A, User Information, pp. A5.16–A6.40.
- [20] Schreurs, P., Veldpau, F., and Brekelmans, W., 1986, "Simulation of Forming Processes Using the Arbitrary Eulerian-Lagrangian Formulation," *Comput. Methods Appl. Mech. Eng.*, **58**, pp. 19–36.
- [21] Huétink, J., Vreede, P., and van der Lugt, J., 1990, "Progress in Mixed Eulerian-Lagrangian Finite Element Simulation of Forming Processes," *Int. J. Numer. Methods Eng.*, **30**, pp. 1441–1457.
- [22] Goijaerts, A., Stegeman, Y., Govaert, L., Brokken, D., Brekelmans, W., and Baaijens, F., 1998, "A validated fem model to improve metal blanking," *Simulation of Materials Processing: Theory, Methods and Applications*, Twente, pp. 979–984.
- [23] Freudenthal, A. M., 1950, *The Inelastic Behavior of Solids*, Wiley, New York.
- [24] Cockroft, M. G., and Latham, D. J., 1968, "Ductility and the Workability of Metals," *J. Inst. Met.*, **96**, pp. 33–39.
- [25] Jeong, S., Kang, J., and Oh, S., 1996, "A Study on Shearing Mechanism by FEM Simulation," *Advanced Technology of Plasticity*, Columbus, Ohio, USA, pp. 631–634.
- [26] Klocke, F., and Sweeney, K., 1998, "Crack Prediction and Prevention in the Fine Blanking Process: FEM Simulations and Experimental Results," *Proceedings of the International Conference on Sheet Metal Forming*, Twente, pp. 215–222.
- [27] Faura, F., Garcia, A., and Estrems, M., 1998, "Finite Element Analysis of Optimum Clearance in the Blanking Process," *J. Mater. Process. Technol.*, **80–81**, pp. 121–125.
- [28] Oyane, M., Sato, T., Okimoto, K., and Shima, S., 1980, "Criteria for ductile fracture and their applications," *J. Mech. Work. Technol.*, **4**, pp. 65–81.
- [29] Rice, J. R., and Tracey, D. M., 1969, "On the Ductile Enlargement of Voids in Triaxial Stress Fields," *J. Mech. Phys. Solids*, **17**, pp. 201–217.
- [30] Goijaerts, A. M., Govaert, L. E., and Baaijens, F. P. T., 2000, "Evaluation of Ductile Fracture Models for Different Metals in Blanking," submitted to *J. Mater. Process. Technol.*
- [31] Goijaerts, A. M., Govaert, L. E., and Baaijens, F. P. T., 2000, "Experimental and Numerical Investigation on the Influence of Process Speed on the Blanking Process," submitted to *J. Manufacturing Science and Engineering Transactions*.